K-bentonites in the Argentine Precordillera contemporaneous with rhyolite volcanism in the Famatinian Arc

C. M. FANNING[1], R. J. PANKHURST[2], C. W. RAPELA[3], E. G. BALDO[4], C. CASQUET[5] & C. GALINDO[5]

[1]*Research School of Earth Sciences, The Australian National University, Canberra A.C.T. 0200, Australia*
[2]*British Geological Survey, Keyworth, Nottingham NG12 5GG, UK*
[3]*Centro de Investigaciones Geológicas, Universidad Nacional de La Plata, La Plata, Argentina*
[4]*Departamento de Geología, Universidad Nacional de Córdoba, Córdoba, Argentina*
[5]*Departamento de Petrología y Geoquímica, Universidad Complutense, 28040 Madrid, Spain*

Abstract: New U–Pb radiometric dates for K-bentonite horizons within the Lower Cambrian to Middle Ordovician platform carbonates from the Precordillera terrane of NW Argentina provide further constraints on models for the allochthonous or parautochthonous accretion of this terrane. Two K-bentonite layers from the Talacasto section yield indistinguishable sensitive high-resolution ion microprobe (SHRIMP) U–Pb zircon dates of 469.5 ± 3.2 Ma and 470.1 ± 3.3 Ma respectively. These are within uncertainty of the U–Pb SHRIMP zircon date of 468.3 ± 3.4 Ma for a porphyritic rhyolite from the Famatinian magmatic arc, Sierra de las Planchadas, near Rio Chaschuil. Geochemical and isotope data also demonstrate the similarity of the K-bentonite and Chaschuil rhyolite parent magmas. Thus, it is highly probable that the Famatinian arc volcanoes provided the ash for the K-bentonite horizons, suggesting proximity to the Precordillera terrane during the deposition of the Lower Cambrian to Middle Ordovician platform carbonates. This implication supports a mid-Ordovician collision model, but could also be compatible with a parautochthonous model for docking of the Precordillera terrane, by movement along the Pacific margin of Gondwana, rather than across the Iapetus Ocean.

Keywords: U–Pb, SHRIMP, Ordovician, Gondwana, terranes.

The Argentine Precordillera (Fig. 1) has become widely regarded as one of the best-documented examples of an accreted terrane, at least in South America (e.g. Thomas & Astini 2003). However, its suggested Laurentian origin has been disputed in other models to explain the apparent inconsistencies of this terrane in a Gondwana context, including the parautochthonous model (e.g. Baldis *et al.* 1989; Finney *et al.* 2003*a*).

This region, immediately east of the Andean Cordillera at 28 32°S, is notable for a Palaeozoic stratigraphy that contrasts with that of the neighbouring areas of Gondwana. In particular, the lowest exposed rocks are Lower Cambrian to Middle Ordovician platform limestones (e.g. Astini *et al.* 1995) with fossil faunas that have been described as showing a time progression from Laurentian to Gondwanan types (e.g. Benedetto 1998). To the west of the carbonate platform a continental rise with turbidites and ocean-floor mafic and ultramafic rocks was present during the Ordovician, and the carbonate sequence is unconformably overlain by an Upper Ordovician to Devonian arenaceous succession (Astini *et al.* 1995; Astini 1998). Evidence for the presence of a Grenville-age metamorphic basement to the Lower Palaeozoic Precordillera successions comes from the dating of amphibolite xenoliths in Miocene intrusive rocks (Abruzzi *et al.* 1993). To the east of the Precordillera, Lower Palaeozoic rocks are largely igneous in nature, with the development of intense magmatism of continental margin calc-alkaline type during the Ordovician. A broad belt, the Famatinian magmatic arc (Fig. 1), extends from about 26°S to 33°S, and was apparently developed on and within a basement of metasediments and gneisses. These basement rocks contain zircons with ages in the range *c.* 500 to *c.* 2000 Ma and have Mesoproterozoic Nd-model ages indicating that the protolith rocks were derived from Proterozoic to Cambrian sources (e.g. Pankhurst *et al.* 1998; Rapela *et al.* 2001). Together with detailed changes in palaeontology and sedimentology of the Precordillera, this has led to models in which the Precordillera terrane collided with the supercontinent of Gondwana in Mid-Ordovician (e.g. Casquet *et al.* 2001; Thomas & Astini 2004), or Silurian (Keller 1999) times. However, some recent tectonic and correlation studies have cast doubt on the allochthonous Laurentian origin of the Precordillera, suggesting instead supercontinent-parallel movement of terrane slices from southern Gondwana (Aceñolaza *et al.* 2002).

K-bentonite horizons, interpreted as altered volcanic infall, are interbedded with the limestones of the Precordillera and have been taken as evidence of felsic volcanism contemporaneous with carbonate sedimentation (Fig. 2). Huff *et al.* (1997) presented U Pb multi-grain zircon data indicating a Mid-Ordovician age of 464 ± 2 Ma for one of these K-bentonite horizons. It was further suggested by Bergstrom *et al.* (1996) that these K-bentonites represent felsic igneous activity related to collision tectonism. However, Huff *et al.* (1998) showed that the detailed stratigraphy of the K-bentonites in the Precordillera does not correspond to that exhibited in the Ordovician of eastern North America or Europe, so that the possibility of a source for the volcanic ashes within Gondwana should be considered. Consequently, we have carried out U Pb sensitive high-resolution ion microprobe (SHRIMP) dating of zircons from classic localities of the K-bentonites and possible equivalents in the Famatinian arc to provide further constraints on the age and source of the Precordillera volcanic horizons, and on the implications for the origin of this terrane.

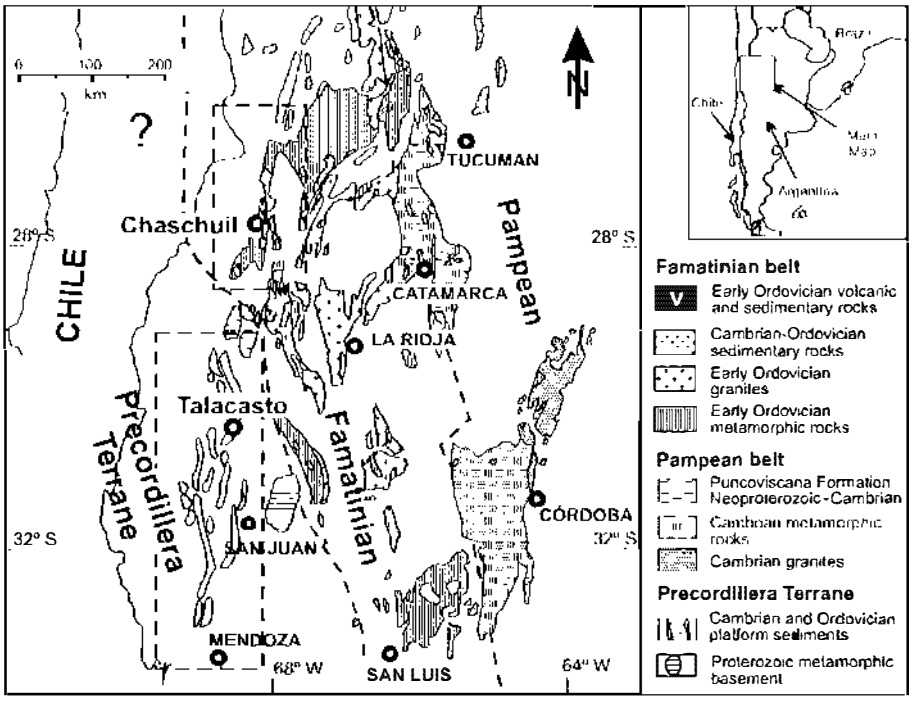

Fig. 1. Geological sketch map of NW Argentina showing the regional context of this study.

Famatinian volcanism

The Famatinian magmatic belt of the Sierras Pampeanas, Puna and Eastern Cordillera constitutes the largest Early Palaeozoic igneous province in South America. Most tectonic interpretations (e.g. Rapela *et al.* 1992; Toselli *et al.* 1996) suggest emplacement in a Late Cambrian to Mid-Ordovician continental margin arc. Famatinian magmatism is dominated by I- and S-type granitic rocks, with U–Pb ages mostly in the range *c.* 470–500 Ma (Pankhurst *et al.* 2000). Ordovician volcanic and volcaniclastic successions crop out in the NW sector of the Sierra de Famatina and the Puna (Rapela *et al.* 1992; Mannheim & Miller 1996; Saavedra *et al.* 1998; Astini & Dávila 2002). The petrology and geochemistry of these volcanic rocks show that they form an essentially bimodal association of basalt and subalkaline rhyolite, with less common intermediate compositions (Mannheim & Miller 1996). Associated volcaniclastic rocks are interbedded with Arenig to Llanvirn shallow marine sediments (Albanesi & Vaccari 1994; Mángano & Buatois 1996; Toro & Brussa 1997). The depositional facies are consistent with penecontemporaneous, explosive volcanism (Mángano & Buatois 1996; Mannheim & Miller 1996).

Samples

K-bentonites were sampled from the San Juan limestone in the Talacasto section (Fig. 2), where their spatial distribution, stratigraphic position and mineralogical composition have been described in detail (Bergstrom *et al.* 1996; Huff *et al.* 1998). Two samples (TAL 6071: 31°00′34.3″S, 68°46′16.1″W; TAL 6073: 31°01′35.0″S, 68°45′04.6″W) were taken from below the *A variabilis* conodont zone (Lozano & Hünicken 1990; Bergstrom *et al.* 1996). Although the samples were taken from localities 1 km apart, their exact relative stratigraphic positions are difficult to define because of isoclinal folding and possible repetition of the sequence. The samples are both buff- to tan-coloured bentonitic clays.

Samples of Famatinian rhyolite were collected from the Sierra de Las Planchadas, near Río Chaschuil (27°47′44.1″S, 68°03′10.0″W). The Palaeozoic geology of this area has been described by Cisterna (2001), who considered the volcanic rocks to be interbedded, and therefore partially coeval, with marine sediments of the Suri Formation (Fig. 3) (Albanesi & Vaccari 1994; Mángano & Buatois 1996; and discussion below). Sample CHA 3008 is a porphyritic rhyolite, with 0.5–4 mm phenocrysts of euhedral plagioclase (An_{32}) and corroded quartz in a fine-grained groundmass of quartz, alkali-feldspar and plagioclase. The lithological association of the lavas includes heterogeneous rhyolite breccias bearing spherulitic lithoclasts and leucocratic subvolcanic domes. Sample CHA 3005 was taken from one of these rhyolite domes; it has miarolitic cavities and a conspicuous graphic and granophyric fabric.

Analytical methods

Heavy mineral concentrates were prepared from the porphyritic rhyolite (CHA 3008) total rock sample using standard crushing, desliming, heavy liquid (specific gravity 2.96 and 3.3) and paramagnetic procedures. The K-bentonite samples did not require crushing; instead the samples were rolled and then the total clay-rich sample was deflocculated and deslimed by continuous washing under gently running water. A heavy mineral concentrate was then prepared following standard heavy liquid and paramagnetic procedures. Zircons were hand-picked from the mineral separates, mounted in epoxy together with chips of reference zircons FC1 and SL13, ground approximately halfway through and polished. Reflected and transmitted light photomicrographs and cathodoluminescence (CL) SEM images were prepared for all zircons. The CL images were used to decipher the internal structures of the sectioned grains and to target specific areas within the zircons.

U–Th–Pb zircon analyses were made using SHRIMP II, each analysis consisting of six scans through the mass range following procedures as described by Williams (1998, and references therein). The data were reduced using the SQUID Excel Macro of Ludwig (2000). Pb/U ratios were normalized relative to a value of 0.1859 for the $^{206}Pb/^{238}U$ ratio of the FC1 or AS3 Duluth Gabbro reference zircons, equivalent to an age of 1099 Ma (see Paces & Miller 1993). Uncertainties given for individual analyses (ratios and ages) are at the 1σ level, but the uncertainties in calculated weighted mean ages are reported as 95% confidence limits and include the uncertainty in the reference zircon U/Pb ratio calibration (Table 1). Tera & Wasserburg (1972) concordia plots, probability density plots with stacked histogram, and weighted mean $^{206}Pb/^{238}U$ age calcula-

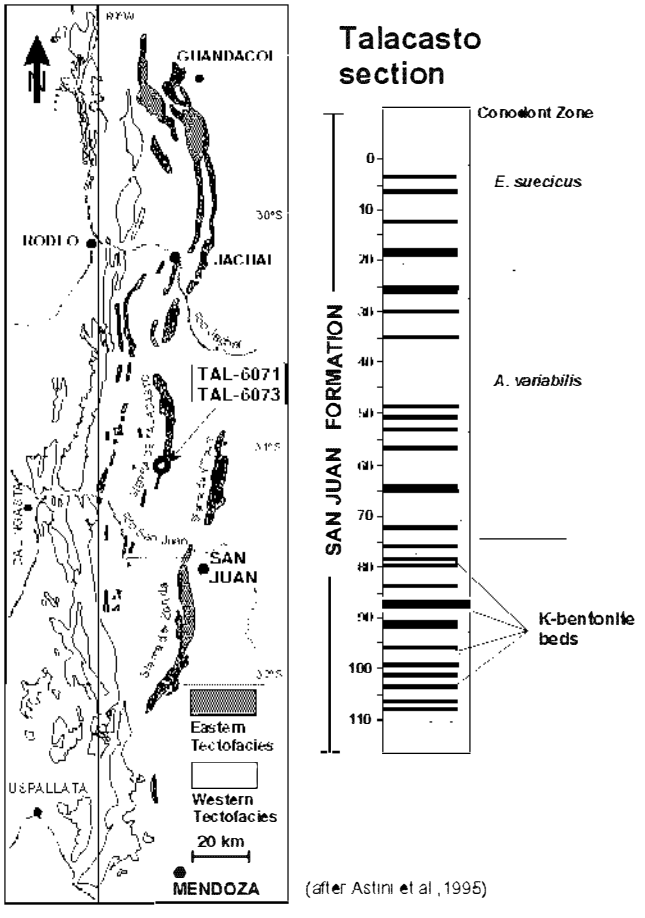

Fig. 2. Sketch map of Cambro-Ordovician limestone outcrops in the Argentine Precordillera and stratigraphic section of the San Juan Formation in the Talacasto section, showing sampling locality.

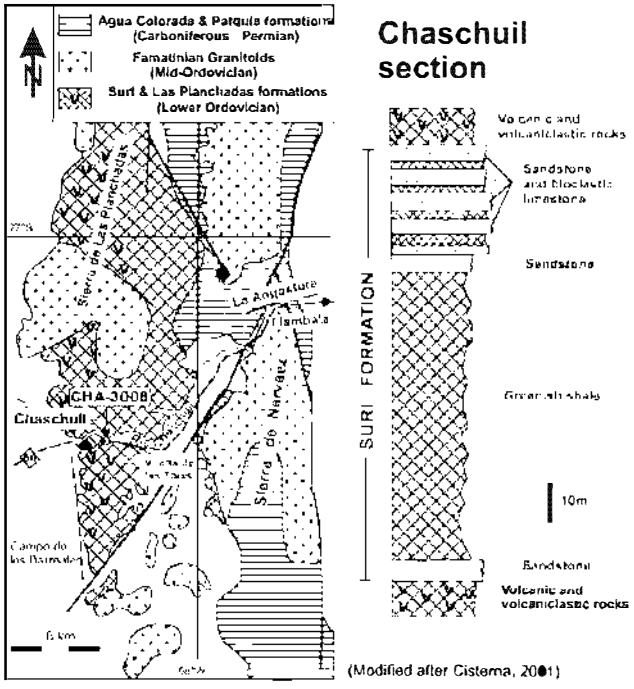

Fig. 3. Sketch map of part of the northern section of the Famatinian magmatic arc and illustrative section of the stratigraphy at Chaschuil, showing sampling locality.

tions were carried out using Isoplot/Ex (Ludwig 1999). The decay constants used are those recommended by the IUGS Subcommission on Geochronology (Steiger & Jäger 1977).

Both samples of the Chaschuil rhyolites were analysed for major and trace elements at ACTLABS, Canada. The results were compared with a more regional study of Famatinian volcanism (Mannheim & Miller 1996), and with K-bentonite analyses from the Precordillera (Huff *et al.* 1998)

U–Pb results

Sample TAL 6071

The zircons from this sample are euhedral, relatively equant, small grains, many less than 100 μm in length with length to breadth ratios of ⩽3:1. The grains in general have bipyramidal terminations. There is no evidence for significant transport, such as rounding or pitting of the external surfaces (Fig. 4a) and the CL images reveal a dominant simple, centre to rim, zoned internal structure. Some grains are more lozenge shaped in section and the CL images suggest that such grains may have discordant central areas of possible inherited components.

Twenty-four analyses were made on 23 grains (Table 1). The analysis of the lower-U grain 5 is anomalous, with a Cenozoic $^{206}Pb/^{238}U$ age. This grain has a completely different internal CL structure, being very bright and showing no internal zonation at the same relative level of contrast as all the other grains. The grain is thought to be a contaminant and so will not be considered further in this discussion.

On a Tera–Wasserburg concordia plot (Fig. 4a), the other 23 analyses form a dispersed grouping low in common Pb, near or within uncertainty of the concordia curve. The slight dispersion is further highlighted on a probability density plot (with stacked histogram) of the radiogenic $^{206}Pb/^{238}U$ ages. Although there is a dominant group at about 470 Ma, the relative probability curve tails off to both the older and younger sides. A weighted mean of all 23 analyses has excess scatter about a mean of *c.* 470 Ma (MSWD = 3.6). The tailing displayed on the relative probability plot is due to only three analyses on the younger side; analyses 4.1 and 12.1 with $^{206}Pb/^{238}U$ ages of *c.* 455 Ma and *c.* 450 Ma. On the older side there are two analyses forming that 'tail'; analysis 3.1 has a $^{206}Pb/^{238}U$ age of *c.* 480 Ma and 20.1 of *c.* 485 Ma. One may consider these five areas to respectively reflect radiogenic Pb loss and subtle inheritance. A weighted mean of the $^{206}Pb/^{238}U$ ages for the remaining 18 analyses has no excess scatter, giving 469.5 ± 3.2 Ma (MSWD = 1.13, 95% confidence limits), and this is interpreted to be the crystallization age of the zoned magmatic zircon.

Sample TAL 6073

The zircons from this sample are similar to those from sample TAL 6071; that is, they are small, euhedral, relatively equant grains with bipyramidal terminations and little evidence for surficial transport (Fig. 4b). Although most are less than 100 μm in length, with length to breadth ratios of ⩽3:1, there are some more elongate grains in this sample. Rare, elongate subround grains are also present (e.g. grain 19). The CL images reveal a dominantly simple zoned internal structure, although there are

Table 1. *U–Pb zircon SHRIMP data*

Grain.spot	U (ppm)	Th (ppm)	Th/U	$^{206}Pb^{*}$ (ppm)	$^{204}Pb/^{206}Pb$	f_{206} (%)	Total				Radiogenic		Age (Ma)	
							$^{238}U/^{206}Pb$	±	$^{207}Pb/^{206}Pb$	±	$^{206}Pb/^{238}U$	±	$^{206}Pb/^{238}U$	±
TAL 6071														
1.1	199	88	0.44	12.7		0.02	13.484	0.157	0.0564	0.0009	0.0741	0.0008	461.1	4.8
2.1	149	72	0.48	9.8		0.05	13.082	0.189	0.0570	0.0010	0.0764	0.0011	474.6	6.7
3.1	206	111	0.54	13.7		<0.01	12.908	0.156	0.0562	0.0009	0.0775	0.0008	481.3	4.8
4.1	139	67	0.49	8.7		0.09	13.612	0.181	0.0568	0.0011	0.0734	0.0008	456.6	5.0
5.1	153	110	0.72	0.4		1.09	349.6	9.9	0.0550	0.0054	0.0028	0.0001	18.2	0.5
6.1	189	116	0.61	12.1	0.000117	0.04	13.101	0.155	0.0568	0.0009	0.0763	0.0008	474.0	4.8
7.1	193	89	0.46	12.6	0.000092	<0.01	13.216	0.155	0.0558	0.0009	0.0757	0.0008	470.6	4.7
8.1	152	72	0.48	10.0		<0.01	12.972	0.149	0.0560	0.0010	0.0772	0.0009	479.1	5.1
9.1	116	54	0.47	7.4	0.000107	0.20	13.365	0.157	0.0579	0.0012	0.0747	0.0009	464.2	5.4
10.1	161	77	0.48	10.4	0.000136	0.05	13.262	0.154	0.0568	0.0010	0.0754	0.0010	468.4	5.9
11.1	197	122	0.62	12.6	0.000167	<0.01	13.421	0.157	0.0555	0.0009	0.0746	0.0008	463.7	4.7
12.1	221	138	0.62	13.9	0.000049	0.21	13.699	0.158	0.0577	0.0009	0.0728	0.0007	453.3	4.4
13.1	224	133	0.59	14.3	0.000151	<0.01	13.243	0.151	0.0564	0.0008	0.0755	0.0008	469.3	4.8
13.2	250	158	0.64	15.5		0.27	13.804	0.154	0.0582	0.0008	0.0722	0.0007	449.7	4.3
14.1	190	85	0.45	12.2		<0.01	13.392	0.158	0.0558	0.0009	0.0747	0.0008	464.8	4.7
15.1	175	83	0.47	11.3	0.000472	0.55	13.307	0.171	0.0608	0.0010	0.0747	0.0010	464.6	5.9
16.1	307	176	0.57	19.9	0.000117	0.06	13.239	0.126	0.0569	0.0007	0.0755	0.0007	469.1	4.3
17.1	402	218	0.54	25.9	0.000015	0.01	13.322	0.123	0.0564	0.0006	0.0751	0.0007	466.6	4.1
18.1	186	93	0.50	12.3		<0.01	12.980	0.153	0.0550	0.0009	0.0772	0.0008	479.4	4.8
19.1	261	135	0.52	17.1	0.000035	<0.01	13.140	0.128	0.0562	0.0008	0.0761	0.0007	473.0	4.5
20.1	225	131	0.58	15.2	0.000096	0.10	12.732	0.127	0.0577	0.0010	0.0785	0.0008	487.0	4.8
21.1	255	158	0.62	16.6	0.000034	0.01	13.176	0.128	0.0566	0.0008	0.0759	0.0007	471.8	4.4
22.1	144	64	0.44	9.3	0.000138	0.03	13.365	0.188	0.0566	0.0010	0.0748	0.0011	465.0	6.4
23.1	206	146	0.71	13.5		0.07	13.142	0.150	0.0571	0.0009	0.0760	0.0008	472.4	4.7
TAL 6073														
1.1	201	112	0.55	12.6	0.000163	0.07	13.638	0.147	0.0567	0.0009	0.0733	0.0008	455.8	4.8
2.1	140	96	0.68	9.0	0.000076	0.13	13.358	0.148	0.0574	0.0015	0.0748	0.0009	464.8	5.2
3.1	309	214	0.69	19.2	0.000364	0.97	13.802	0.139	0.0637	0.0008	0.0717	0.0007	446.7	4.2
4.1	135	80	0.59	8.8	0.000277	<0.01	13.118	0.167	0.0555	0.0011	0.0763	0.0010	474.2	5.9
5.1	599	248	0.41	38.6	0.000390	0.90	13.546	0.116	0.0633	0.0006	0.0732	0.0006	455.2	3.9
6.1	104	50	0.48	6.8	0.000288	0.35	13.207	0.163	0.0592	0.0013	0.0755	0.0009	468.9	5.6
7.1	144	76	0.52	9.3	0.000312	<0.01	13.377	0.148	0.0559	0.0010	0.0748	0.0008	465.0	5.1
8.1	266	166	0.63	17.0	0.000086	0.03	13.448	0.129	0.0565	0.0008	0.0743	0.0007	462.2	4.4
9.1	261	183	0.70	16.8	0.000076	<0.01	13.346	0.169	0.0560	0.0008	0.0750	0.0009	466.0	5.5
10.1	149	68	0.45	9.7	0.000062	<0.01	13.190	0.144	0.0564	0.0010	0.0758	0.0008	471.1	5.0
11.1	129	68	0.53	8.4	0.000245	0.14	13.243	0.156	0.0576	0.0011	0.0754	0.0009	468.6	5.2
12.1	148	63	0.43	9.5	0.000006	0.64	13.335	0.165	0.0615	0.0011	0.0745	0.0008	463.3	5.3
13.1	113	54	0.48	7.7	0.000293	0.02	12.532	0.147	0.0572	0.0012	0.0798	0.0010	494.8	5.7
13.2	302	204	0.68	20.0	0.000091	0.10	12.962	0.161	0.0575	0.0007	0.0771	0.0010	478.6	5.8
14.1	154	74	0.48	10.1		0.05	13.086	0.141	0.0570	0.0010	0.0764	0.0008	474.5	5.0
15.1	176	82	0.47	11.6	0.000183	<0.01	13.101	0.137	0.0556	0.0009	0.0764	0.0008	474.7	4.8
16.1	99	48	0.49	6.3	0.000327	0.19	13.417	0.154	0.0578	0.0013	0.0744	0.0009	462.5	5.5
17.1	95	53	0.56	5.9	0.000597	0.99	13.974	0.171	0.0637	0.0014	0.0709	0.0009	441.3	5.4
18.1	97	49	0.51	6.3		<0.01	13.299	0.164	0.0554	0.0016	0.0753	0.0010	467.9	5.7
19.1	178	139	0.78	13.3		0.10	11.496	0.117	0.0590	0.0009	0.0869	0.0009	537.2	5.4
19.2	151	128	0.85	10.1	0.000332	0.81	12.888	0.157	0.0633	0.0010	0.0770	0.0008	478.0	5.0
19.3	226	223	0.99	16.4		0.25	11.832	0.115	0.0599	0.0008	0.0843	0.0008	521.8	5.0
20.1	43	82	1.89	2.7	0.000799	0.35	13.699	0.227	0.0588	0.0020	0.0727	0.0012	452.7	7.4
21.1	147	115	0.78	9.7		0.14	13.044	0.142	0.0578	0.0010	0.0766	0.0009	475.5	5.1
22.1	279	326	1.17	18.1	0.003532	10.34	19.814	0.192	0.1350	0.0027	0.0452	0.0008	285.1	5.0
23.1	67	41	0.61	4.4	0.000018	0.01	13.028	0.255	0.0567	0.0015	0.0767	0.0014	476.7	8.4
24.1	171	90	0.53	11.3		<0.01	13.075	0.158	0.0565	0.0009	0.0765	0.0008	475.2	4.9
CHA 3008														
1.1	350	221	0.63	22.7	0.000408	0.23	13.263	0.157	0.0582	0.0008	0.0752	0.0009	467.6	5.4
2.1	242	121	0.50	15.8	0.000256	0.43	13.157	0.163	0.0599	0.0010	0.0757	0.0010	470.3	5.7
3.1	478	296	0.62	31.1	0.000257	0.26	13.197	0.169	0.0585	0.0007	0.0756	0.0010	469.7	5.9
4.1	468	272	0.58	29.8	0.000074	0.25	13.478	0.153	0.0582	0.0007	0.0740	0.0009	460.3	5.1
5.1	570	328	0.58	37.1	0.000116	0.30	13.199	0.164	0.0589	0.0006	0.0755	0.0010	469.4	5.7
6.1	343	180	0.52	22.1	0.000341	0.29	13.324	0.157	0.0587	0.0008	0.0748	0.0009	465.2	5.4
7.1	365	204	0.56	23.5	0.000200	0.34	13.352	0.156	0.0590	0.0008	0.0746	0.0009	464.1	5.3
8.1	361	252	0.70	23.6	0.000129	0.17	13.159	0.175	0.0579	0.0008	0.0759	0.0010	471.4	5.9
9.1	371	199	0.54	24.2	0.000204	0.19	13.165	0.177	0.0581	0.0008	0.0758	0.0010	471.1	5.9
10.1	425	274	0.64	27.9	0.000171	0.06	13.105	0.153	0.0570	0.0007	0.0763	0.0009	473.8	5.3
11.1	340	186	0.55	22.1	0.000177	0.26	13.206	0.158	0.0586	0.0009	0.0755	0.0009	469.4	5.4
12.1	431	262	0.61	27.9	0.000081	0.33	13.284	0.152	0.0590	0.0007	0.0750	0.0009	466.4	5.2
13.1	334	193	0.58	21.8	0.000190	0.13	13.139	0.169	0.0576	0.0010	0.0760	0.0009	472.3	5.6
14.1	370	214	0.58	23.9	0.000249	0.24	13.272	0.155	0.0583	0.0009	0.0752	0.0009	467.2	5.4
15.1	430	304	0.71	27.9	0.000179	0.14	13.211	0.150	0.0576	0.0008	0.0756	0.0009	469.7	5.5

Uncertainties given at the 1σ level. Error in FC1 reference zircon calibration was 0.48% (at 95% confidence
in AS3 reference zircon calibration was 0.40% (at 95% confidence limit) for the analytical session for CHA 3008 (not included in above errors but required when comparing data from different mounts) –, no 204Pb was detected f_{206} %, percentage of ^{206}Pb that is common Pb. Correction for common Pb made using the measured $^{238}U/^{206}Pb$ and $^{207}Pb/^{206}Pb$ ratios following Tera & Wasserburg (1972), as outlined by Williams (1998; the so-called ^{207}Pb correction method).

some grains that appear to have inherited centre components (Fig. 4b).

Twenty-seven analyses were made on 24 grains (Table 1). The U concentrations are notably lower than that of the other sample, ranging from *c.* 70 to 600 ppm, with most less than 200 ppm. The analysis of grain 22 is significantly enriched in common Pb, has a $^{206}Pb/^{23}$

discordant. Three analyses were made on grain 19, a complexly structured grain interpreted to have a zoned magmatic rim to a possible older, less structured core. Two analyses of the near-edge areas yield Cambrian $^{206}Pb/^{23}$

(analyses 19.1 and 19.3). A third analysis (19.2) is of a highly

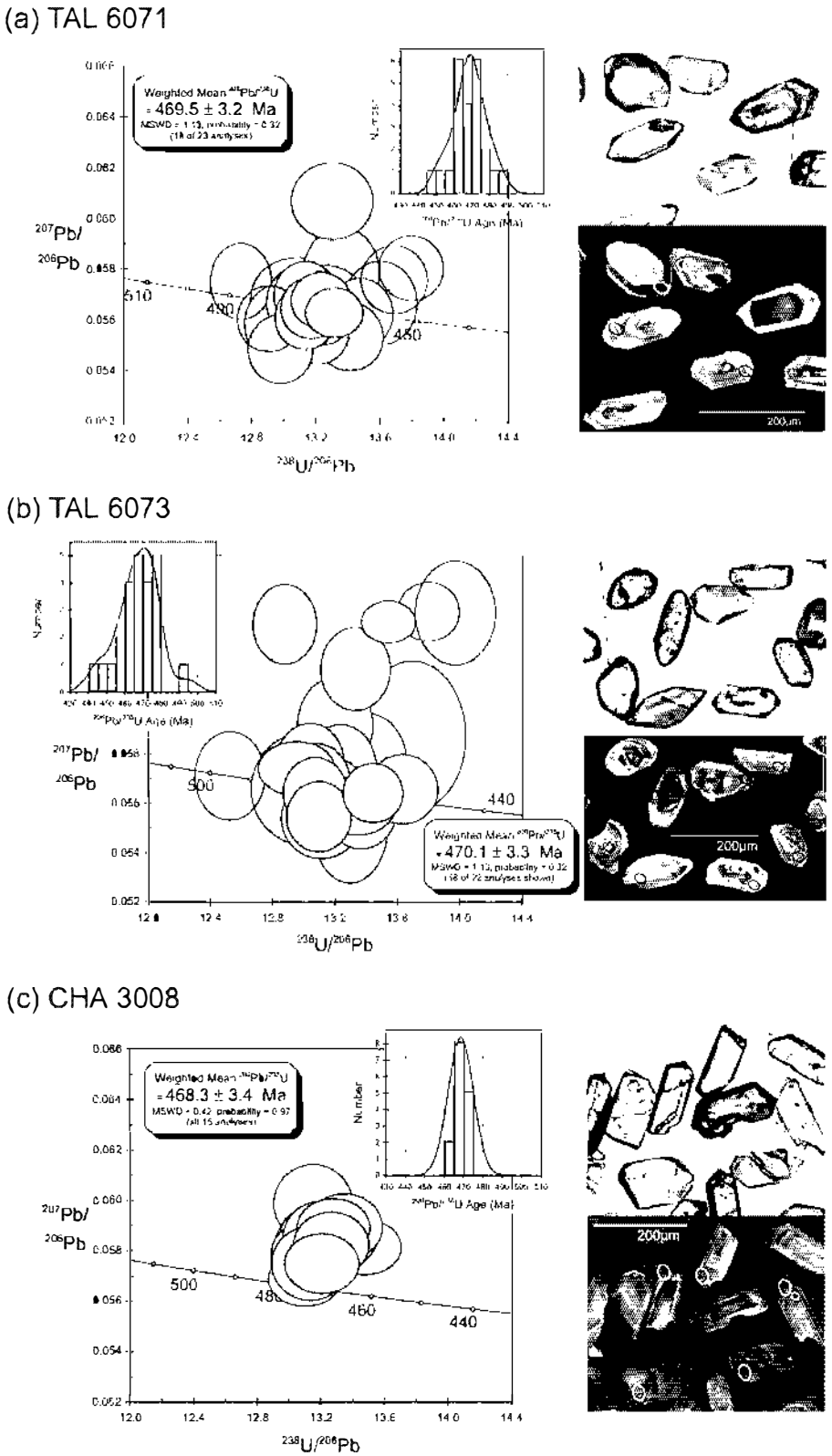

Fig. 4. Tera Wasserburg plots of U Pb SHRIMP data for zircons from K-bentonites from the Talacasto section of the Argentine Precordillera (TAL 6071, TAL 6073) and the Chaschuil rhyolite from the northern Famatinian magmatic belt (CHA 3008) together with probability density plots. Shaded portions show the data used in calculating the ages (total ratios plotted with error ellipses at 68% confidence level; age errors at 95%). Panels at the right show transmitted light photomicrographs and SEM CL images of the same selection of representative grains.

cracked edge region, but records a $^{206}Pb/^{238}U$ age of *c.* 475 Ma, similar to other interpreted magmatic zircon areas analysed from this sample.

The remaining 20 analyses form a slightly dispersed grouping on a Tera–Wasserburg concordia plot (Fig. 4b), the analyses being mostly low in common Pb, at about 470 Ma. The probability density plot with stacked histogram highlights the dispersion in $^{206}Pb/^{238}U$ ages, showing a skew mostly towards the young end of the age spectrum, although with a slight tail at the high end because of analysis 13.1. Analyses 3.1, 17.1 and 20.1 all have slightly younger $^{206}Pb/^{238}U$ ages of *c.* 445, *c.* 440 and *c.* 450 Ma, respectively; analyses 3.1 and 17.1 are more

enriched in common Pb and the young ages are interpreted as resulting from radiogenic Pb loss. If these three analyses, plus the slightly older 13.1 are excluded, the weighted mean $^{206}Pb/^{23}$ Analysis 5.1 shows a similar enrichment in common Pb to analyses 3.1 and 17.1 that are interpreted to have lost radiogenic Pb. Analysis 5.1 has a $^{206}Pb/^{238}U$ age of *c.* 455 Ma, as does the analysis of grain 1. If these two analyses are also excluded from the weighted mean age calculation, the resultant $^{206}Pb/^{238}$

Sample CHA 3008

The zircons from this sample are euhedral elongate grains with bipyramidal terminations, or fragments of such grains. Some grains are thin and very elongate, with length to breadth ratios up to 6:1. A few grains have longitudinal internal cavities consistent with trapped vapour phases during rapid cooling in a volcanic to subvolcanic setting. The CL images reveal an internal structure of simple, core to rim, oscillatory zonation (Fig. 4c).

For this study, 15 grains were analysed. All 15 analyses are low in common Pb and the Tera Wasserburg plot of the total ratios (Fig. 4c) shows that they form a tight cluster within uncertainty of the concordia curve. On a probability density plot of the $^{206}Pb/^{238}$ analyses form a simple bell-shaped curve and the weighted mean has no excess scatter, giving 468.3 ± 3.4 Ma. This is interpreted as the crystallization age of the simple zoned magmatic zircon from sample CHA 3008.

The age of K-bentonite volcanism

The two results for the Talacasto K-bentonites yield a mean of 469.8 ± 2.3 Ma. The new age is slightly older than the conventional U Pb zircon age of 464 ± 2 Ma reported by Huff *et al.* (1997) for a K-bentonite from Cerro Viejo, stratigraphically constrained to the base of the Darriwilian stage (Mid-Ordovician). However, their age was derived by regressing three almost concordant data points with one very discordant one (with a $^{207}Pb/^{206}Pb$ age of 800 Ma). Our analysis of their data using Isoplot/Ex gives a lower intercept of 463.1 ± 5.8 Ma (2σ error) but with an MSWD of 3.3. If the discordant point is disregarded, the mean $^{206}Pb/^{23}$ (MSWD = 8.4) whereas the mean $^{207}Pb/^{206}Pb$ age is 470.9 ± 3.4 Ma (MSWD = 0.2). The last of these results seems to be the most robust, and is in agreement with the SHRIMP U Pb results.

In stratigraphic terms, our K-bentonite ages fall within the pre-Darriwilian stage of the Mid-Ordovician (not formally named) according to the 2002 IUGS International Stratigraphic Chart (or Arenig according to the GSA 1999 Geologic Time Scale, where the Arenig Llanvirn boundary is at 470 Ma). A late Arenig Llanvirn age attribution is consistent with the Early Mid-Whiterockian stratigraphic age of this part of the San Juan limestone based on the conodont evidence (Bergstrom *et al.* 1996).

The age obtained for the Chaschuil rhyolite falls at the young end of the age range published for Famatinian plutonism (Pankhurst *et al.* 2000). According to the 2002 IUGS International Stratigraphic Chart, it is Mid-Ordovician, just before the Darriwilian stage, which would translate as latest Arenig (or perhaps earliest Llanvirn according to the GSA time scale). This would be in agreement with the work of Cisterna (2001), who suggested that the volcanism of the Las Planchadas Formation was partially coincident with deposition of the Suri Formation, and hence of Arenig age. However, an early Llanvirn age would conform better to the views of other workers (e.g. Mángano & Buatois 1996), who have usually regarded the volcanic rocks as unconformably overlying the Suri Formation and thus of Mid-Ordovician age. Astini & Dávila (2002) have also proposed that the age of volcanic sedimentary associations in this area extends into the Mid-Ordovician and younger, and that their age is for- ^{8}U age is for- 468 Ma (M mity with the underlying Early Ordovician Famatina Group might represent deformation associated with the collision of the Precordillera terrane.

The age of the K-bentonite event is statistically indistinguishable from the age of the Chaschuil rhyolite. Combining all three gives an overall weighted mean of 469.3 ± 1.9 Ma (MSWD = 0.3). but at the limits of analytical error the data would also allow the K-bentonites to be up to about 5 Ma older than the rhyolite. It should be noted that the K-bentonites within the Precordillera limestone sequences form up to 175 individual horizons, ranging from early Arenig to late Llanvirn in age (Huff *et al.* 1998). The U Pb zircon ages of Famatinian magmatism in the Sierras Pampeanas (mostly plutonic, but probably with volcanic counterparts that have not survived) range over an almost identical interval, from 499 ± 5 Ma to 468 ± 3 Ma (Pankhurst *et al.* 2000). Within this range, most of the earliest magmas belong to a 'behind'-arc tonalite trondhjemite granodiorite suite, and the majority of I- and S-type granites were emplaced in the interval 468 486 Ma. Comparable age ranges were obtained by conventional U Pb dating of plutonic rocks in the northernmost extension of the Famatinian arc (Lork *et al.* 1991; Lork & Bahlburg 1993). Thus, although it may be U ages all 15 coincidental that the Talacasto K-bentonites and Chaschuil rhyolites have such similar ages within this activity, there is no doubt that the magmatism recorded by the ash-falls in the Precordillera are consistently of Famatinian age.

Geochemistry

The new major and trace element data for the Chaschuil rhyolites are presented in Table 2. Both samples are high-silica rhyolites (>75% SiO_2), with 7.4 8.1% $Na_2O + K_2O$, showing normal content of high field strength elements such as Y, Nb, Ta, U and Th, REE patterns with $[La/Yb]_n = 3.6$ 4.5 and negative Eu anomalies ($Eu/Eu^* = 0.48$ 0.55).

Also given in Table 2 is the mean of 12 electron microprobe analyses from Huff *et al.* (1998). Those workers published major ^{8}U age o and trace element (instrumental neutron activation analysis) geochemical data for 'whole-rock' samples of the K-bentonites from Cerro Viejo. As these were necessarily determined on highly altered samples, major element compositions were also determined by electron microprobe on melt inclusions in quartz, which were thought to be representative of the original magma from which the ashes were derived.

The Chaschuil and Cerro Viejo data compare reasonably well; it is clear that both are of typical high-silica rhyolite composition. The total alkali contents are comparable, but the Na_2O/K_2O ratios are >1 in the rhyolite and <1 in the melt inclusions; this may in part be due to the difficulty of determining Na_2O by the electron microprobe method (see Huff *et al.* 1998, p. 115). Aspects of the major element geochemistry are compared in Figure 5. Both Chaschuil and K-bentonite analyses tend to the high-silica rhyolite limit of the field for Famatinian dacites and rhyolites analysed by Mannheim (1993), although individual Na_2O contents were extremely variable in the latter. The TiO_2 v. SiO_2 plot shows the similar close correspondence of the Chaschuil and K-bentonite compositions, falling at the limit of the Famatinian field.

Zr contents of the Chaschuil rhyolites are relatively low (<300 ppm), as are all those of 56 Famatinian dacites and

Table 2. *Geochemistry of Chaschuil rhyolite and Precordillera K-bentonite magma*

	Chaschuil subvolcanic dome CHA 3005	Chaschuil rhyolite CHA 3008	Cerro Viejo K-bentonite* Mean
Major oxides (wt%)			
SiO_2	77.00	75.93	74.18
TiO_2	0.14	0.13	0.10
Al_2O_3	12.09	12.49	11.50
Fe_2O_3	0.40	0.70	–
FeO	1.49	1.46	0.84†
MnO	0.04	0.05	0.04
MgO	0.20	0.55	0.33
CaO	0.52	0.24	0.71
Na_2O	4.48	4.24	3.48
K_2O	2.88	3.81	4.43
P_2O_5	0.03	0.02	0.04
H_2O^+	0.98	0.75	
H_2O	0.23	0.15	
Total	100.48	100.52	95.65

	CHA 3005	CHA 3008		CHA 3005	CHA 3008
Trace elements (ppm)					
Cs	0.3	0.3	La	37.3	33.1
Rb	84	78	Ce	75.0	69.8
Sr	46	44	Pr	9.15	8.43
Ba	575	651	Nd	35.0	33.1
U	3.83	2.84	Eu	1.20	1.38
Th	16.3	14.7	Sm	7.72	7.44
Y	49.6	55.4	Gd	7.46	7.85
Nb	8.1	10.1	Tb	1.38	1.47
Zr	197	206	Dy	8.19	9.15
Hf	5.9	6.3	Ho	1.84	2.06
Ta	0.7	0.8	Tm	0.88	0.98
Ga	14	17	Er	5.68	6.39
			Yb	5.50	6.11
			Lu	0.82	0.90
$^{143}Nd/^{144}Nd$‡				0.512387	0.521403
ε_{Nd470}‡				−1.1	−1.0

Major oxides and trace elements determined by inductively coupled plasma (ICP) and ICP-mass spectrometry, respectively (ACTLABS, Canada). Fe^{2+} determined volumetrically at the Centro de Investigaciones Geológicas, La Plata.
*After Huff *et al.* (1998).
†Total Fe as FeO.

rhyolites analysed by Mannheim (1993) (26–226 ppm). This confirms their uniformly subalkaline character (Leat *et al.* 1986). The Zr contents of the K-bentonites reported by Huff *et al.* (1998) ranged from 160 to 570 ppm, perhaps as a result of mobility of Zr under extreme alteration conditions.

Rare earth abundance patterns are plotted in Figure 6. The Chaschuil rhyolite has a typical calc-alkaline rhyolite signature, with enriched light REE (LREE), a negative Eu anomaly, and fairly flat heavy REE (HREE) abundances. The Cerro Viejo K-bentonite analyses fall in a field that overlaps with the Chaschuil rhyolite pattern, but extends to higher concentrations and, in particular, a higher degree of LREE enrichment. In part this may reflect REE mobility during the heavy alteration of the volcanic ash (SiO_2 concentrations are reduced by this process from *c.* 75% in the melt inclusions to *c.* 50% in the K-bentonites), but the K-bentonite pattern with the lowest LREE contents is almost identical to the Chaschuil rhyolite patterns. We conclude that the Chaschuil rhyolite is very close to the composition of the volcanic magmas from which the Precordillera K-bentonites were derived.

The rhyolites have Rb/ precise initial $^{87}Sr/$

470 Ma (Table 2) suggest a rather less 'evolved' source, or one with a lower contribution of older continental crustal material, than for the majority of Famatinian granites (ε_{Nd} ranges from −4.2 to −7.3; Pankhurst *et al.* 1998).

Discussion

The principal conclusion to be drawn from the data presented here is that, within the limits of error of the determinations, the K-bentonites in the San Juan Formation are essentially contemporaneous with the explosive acid volcanic phase of the Famatinian belt, at about 470 ± 2 Ma. Both events can be interpreted as latest Arenig in age, consistent with the known stratigraphy of their occurrences. According to their stratigraphic assignments, other K-bentonite horizons in the Arenig Llanvirn Precordillera limestone sequences cover almost exactly the main period of Famatinian acid magmatism represented by I- and S-type granites. The major element composition of melt inclusions in K-bentonite quartz is comparable with that of the Chaschuil rhyolite, and the REE pattern of the latter falls within the field S

defined by 'whole-rock' analyses of the K-bentonite ashes. Huff determinati

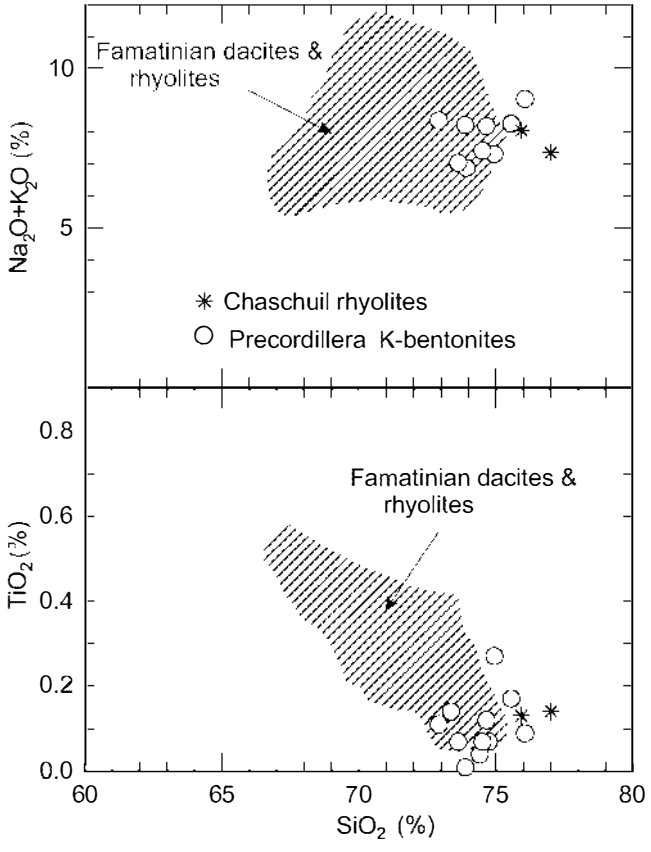

Fig. 5. Plots of (Na_2O + K_2O) and TiO_2 v. SiO_2 for Chaschuil rhyolites (Table 1) and individual analyses of melt inclusions in the Cerro Viejo ignimbrite (Huff *et al.* 1998). The diagonally shaded field for comparison is for Ordovician dacites and rhyolites in the Sierra de Famatina and the Sierra de Las Planchadas (Mannheim 1993).

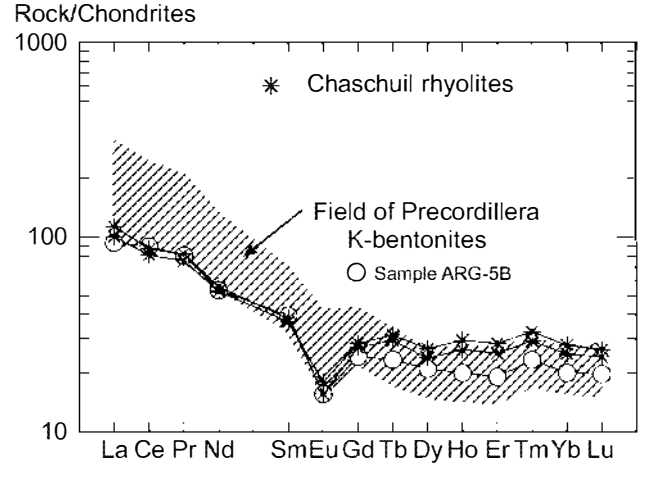

Fig. 6. Rare earth element patterns, normalized to chondrite meteorite abundances, for the Chaschuil rhyolite (asterisks). Equivalent data for K-bentonites from Cerro Viejo, *c.* 70 km north of Talacasto, are shown as a diagonally shaded field, except for one sample (○) that has a pattern almost identical to those of the Chaschuil rhyolite.

et al. (1998) estimated the probable maximum distance of the airborne ash in the K-bentonites from their source as *c.* 200 km. The distance from Talacasto to Chaschuil in the central northern part of the Famatinian belt today is *c.* 275 km, and from Cerro Viejo to Chaschuil *c.* 230 km. These distances obviously do not allow for crustal shortening during Andean deformation, but then they are not perpendicular to the margin: other parts of the Famatinian belt are within 100 km of the K-bentonite outcrops.

More significantly, Finney *et al.* (2003*a*) argued for a much greater separation in the mid-Ordovician, with the Precordillera terrane farther to the SE (present coordinates: Ordovician palaeomagnetic reconstructions show South America rotated through about 180° compared with its present orientation). Consequently, those workers argued for a much later docking event, possibly Devonian collision. In this case the volcanic source would similarly have been far to the SE of Chaschuil, albeit contemporaneous. Pankhurst *et al.* (2003) reported granite boulders of Famatinian age in a Permian conglomerate from southern Patagonia, which suggest extension of the arc to this region.

The argument of Finney *et al.* (2003*b*) is mostly based on the detrital zircon patterns in the Upper Ordovician sandstones of the Precordillera, which are dominated by Neoproterozoic and Mesoproterozoic populations and which lack any input from the marginal Gondwana magmatic arcs (Pampean and Famatinian). They ascribed this to derivation from the interior of Gondwana in a position removed from the reach of Ordovician volcanoes. However, there could be other interpretations consistent with these observations. The Famatinian arc was built on continental basement (Pankhurst *et al.* 1998), and the western Sierras Pampeanas (Pie de Palo, Umango, Maz, Espinal), which lie between the Precordillera sedimentary rocks and the Famatinian arc, contain Mesoproterozoic igneous and metamorphic rocks (e.g. Casquet *et al.* 2001; authors' unpublished U–Pb SHRIMP zircon data). These sierras were formerly thought of as a part of the Grenvillian basement of the Precordillera (the Cuyania terrane or Precordillera terrane), but recent findings suggest that they were probably autochthonous or parautochthonous to Gondwana (Galindo *et al.* 2004). Amalgamation of the Western Sierras Pampeanas with their Grenville-age basement to the Famatinian magmatic arc (e.g. in the Sierra de Valle Fértil) was probably accomplished by 460–470 Ma as suggested by available metamorphic and magmatic ages (Baldo *et al.* 2001; Casquet *et al.* 2001; Rapela *et al.* 2001). This domain of Mesoproterozoic rocks may have thus have been in such a position well before the Late Ordovician and could have been the main source of the detritus in the Precordillera sediments.

Conclusions

On the basis of our new results, we conclude that volcanoes in the Famatinian arc were the source of the volcanic ashes that were converted into the K-bentonites of the San Juan Formation. This would require that the Precordillera was within airborne ash range of the arc by early Arenig times, compatible with collision by Mid-Ordovician times at the latest. Future work on the Precordillera will investigate these propositions with further detrital zircon provenance studies, and also examine the inheritance within existing magmatic zircon suites such as those of the K-bentonites.

This work was supported by grants PB97-1246 and BTE2001-1486, Ministerio de Educación y Cultura, Spain, and grant PICT98-4189, Agencia de Promoción Científica y Tecnológica, Argentina. R.J.P. acknowledges the tenure of a Leverhulme Trust Emeritus Fellowship. This paper is a contribution to International Geological Correlation

Program project 436 (Pacific Gondwana Margin). We thank H. Miller and M. Whitehouse for helpful reviews.

References

ABRUZZI, J.M., KAY, S.M. & BICKFORD, M.E. 1993. Implication for the nature of the Precordilleran basement from the geochemistry and age of Precambrian xenoliths in Miocene volcanic rocks, San Juan province. *XII Congreso Geológico Argentino y II Congreso de Exploración de Hidrocarburos, Mendoza, Actas*, **III**, 331–339.

ACEÑOLAZA, F.J., MILLER, H. & TOSELLI, A.J. 2002. Proterozoic–Early Paleozoic evolution in western South America—a discussion. *Tectonophysics*, **354**, 121–137.

ALBANESI, G.L. & VACCARI, N.E. 1994. Conodontos del Arenigiano en la Formación Suri, Sistema del Famatina, Argentina. *Revista Española de Micropaleontología*, **26**, 125–146.

ASTINI, R.A. 1998. El Conglomerado de Las Vacas y el Grupo Trapiche de la Precordillera: tectónica distensiva en el Ordovícico Tardío. *Revista de la Asociación Geológica Argentina*, **53**, 489–503.

ASTINI, R.A. & DÁVILA, F.M. 2002. El Grupo Cerro Morado (Ordovícico Medio) en el Famatina (28–29°S), Andes centrales del óeste Argentino. *Revista Geológica de Chile*, **29**(2), 241–254.

ASTINI, R.A., BENEDETTO, J.L. & VACCARI, N.E. 1995. The early Paleozoic evolution of the Argentine Precordillera as a Laurentian rifted, drifted and collided terrane: a geodynamic model. *Geological Society of America Bulletin*, **107**, 253–273.

BALDIS, B., PERALTA, S. & VILLEGAS, R. 1989. Esquematizaciones de una posible transcurrencia del terrane de Precordillera como fragmento continental procedente de áreas pampeano-bonaerenses. *Instituto Superior de Correlación Geológica, Tucumán, Argentina*, **5**, 81–100.

BALDO, E., CASQUET, C., RAPELA, C.W., PANKHURST, R.J., GALINDO, C., FANNING, C.M. & SAAVEDRA, J. 2001. Ordovician metamorphism at the southwestern margin of Gondwana: *P–T* conditions and U–Pb SHRIMP ages from Loma de Las Chacras, Sierras Pampeanas. *In: III South American Symposium on Isotope Geology, Extended Abstracts Volume (CD)*. Sociedad Geológica de Chile, Santiago, 544–547.

BENEDETTO, J.L. 1998. Early Palaeozoic brachiopods and associated shelly faunas from western Gondwana: their bearing on the geodynamic history of the pre-Andean margin. *In:* PANKHURST, R.J. & RAPELA, C.W. (eds) *The Proto-Andean Margin of Gondwana*. Geological Society, London, Special Publications, **142**, 57–83.

BERGSTROM, S.M., HUFF, W.D., KOLATA, D.R., KREKELER, M.P.S., CINGOLANI, C.A. & ASTINI, R.A. 1996. Lower and Middle Ordovician K-bentonites in the Precordillera of Argentina: a progress report. *XIII Congreso Geológico Argentino y III Congreso de Exploración de Hidrocarburos, Buenos Aires, Actas*, **V**, 481–490.

CASQUET, C., BALDO, E., PANKHURST, R.J., RAPELA, C.W., GALINDO, C., FANNING, C.M. & SAAVEDRA, J. 2001. Involvement of the Argentine Precordillera Terrane in the Famatinian Mobile Belt: geochronological (U–Pb SHRIMP) and metamorphic evidence from the Sierra de Pié de Palo. *Geology*, **29**(8), 703–706.

CISTERNA, C.E. 2001. Volcanismo subácueo en el Eopaleozoico del Sistema de Famatina, noroeste de Argentina. *Revista de la Asociación Geológica Argentina*, **56**, 16–24.

FINNEY, S., GLEASON, J., GEHRELS, G. & PERALTA, S. 2003a. Post-Ordovician juxtaposition of the Cuyania Terrane and the Famatinian Magmatic Arc. *In: 10th Chilean Geological Congress, Concepción, October 2003* (CD).

FINNEY, S., GLEASON, J., GEHRELS, G., PERALTA, S. & ACEÑOLAZA, G. 2003b. Early Gondwanan connection for the Argentine Precordillera terrane. *Earth and Planetary Science Letters*, **205**, 349–359.

GALINDO, C., CASQUET, C., RAPELA, C., PANKHURST, R.J., BALDO, E. & SAAVEDRA, J. SR 2004. C and O isotope geochemistry and stratigraphy of Precambrian and lower Paleozoic carbonate sequences from the Western Sierras Pampeanas of Argentina: tectonic implications. *Precambrian Research*, **131**, 55–71.

HUFF, W.D., DAVIS, D.W., BERGSTROM, S.M., KREKELER, M.P.S., KOLATA, D.R. & CINGOLANI, C.A. 1997. A biostratigraphically well-constrained K-bentonite U–Pb zircon age of the lowermost Darriwilian stage (Middle Ordovician) from the Argentine Precordillera. *Episodes*, **20**, 29–33.

HUFF, W.D., BERGSTROM, S.M., KOLATA, D.R., CINGOLANI, C.A. & ASTINI, R.A. 1998. Ordovician K-bentonites in the Argentine Precordillera: relations to Gondwana margin evolution. *In:* PANKHURST, R.J. & RAPELA, C.W. (eds) *The Proto-Andean Margin of Gondwana*. Geological Society, London, Special Publications, **142**, 107–126.

KELLER, M. 1999. *Argentine Precordillera: Sedimentary and Plate Tectonic History of a Laurentian Crustal Fragment in South America*. Geological Society of America, Special Paper, **341**.

LEAT, P.T., JACKSON, S.E., THORPE, R.S. & STILLMAN, C.J. 1986. Geochemistry of bimodal basalt–subalkaline/peralkaline rhyolite provinces within the Southern British Caledonides. *Journal of the Geological Society, London*, **143**, 259–273.

LORK, A. & BAHLBURG, H. 1993. Precise U–Pb ages of monazites from the Faja Eruptiva de La Puna Oriental, NW Argentina. *XII Congreso Geológico Argentino y II Congreso de Exploración de Hidrocarburos, Mendoza, Actas*, **IV**, 1–6.

LORK, A., GRAUERT, B., KRAMM, U. & MILLER, H. 1991. U–Pb investigations of monazite and polyphase zircon: implications for age and petrogenesis of trondhjemites of the southern Cordillera Oriental, NW Argentina. *VI Congreso Geológico Chileno, Viña del Mar, Actas*, 398–402.

LOZANO, B. & HÜNICKEN, M.A. 1990. Conodonts and biostratigraphy of the San Juan formation (Arenigian–Llanvirnian) in the Quebrada de Talacasto, Ullum Department, San Juan Province, Argentina. *First Latin American Conodont Symposium, Abstract of Meeting*, 94–96.

LUDWIG, K.R. 1999. *User's Manual for Isoplot/Ex, Version 2.10. A Geochronological Toolkit for Microsoft Excel*. Berkeley Geochronology Center Special Publication, **1a**.

LUDWIG, K.R. 2000. *SQUID 1.00. A User's Manual*. Berkeley Geochronology Center Special Publication, **2**.

MÁNGANO, M.G. & BUATOIS, L. 1996. Estratigrafía, sedimentología y evolución paleoambiental de la Formación Suri en la subcuenca de Chaschuil, Ordovícico del Sistema de Famatina. *In:* ACEÑOLAZA, F., MILLER, H. & TOSELLI, A. (eds) *Geología del Sistema de Famatina*. Münchner Geologische Hefte, Reihe A, **19(6)**, 51–75.

MANNHEIM, R. 1993. Genese der Vulkanite und Subvulkanite des altpaläozischen Famatina-Systems, NW-Argentinien und seine geodynamische Entwicklung. *Munchen Geologische Hefte*, **7**, 1–155.

MANNHEIM,
Famatina-Systems, NW-Argentinien, und seine geodynamische Entwicklung. Münchner Geologische Hefte, **9**.

MANNHEIM, R. & MILLER, H. 1996. Las rocas volcánicas y subvolcánicas del Sistema de Famatina. *In:* ACEÑOLAZA, F., MILLER, H. & TOSELLI, A. (eds) *Geología del Sistema de Famatina*. Münchner Geologische Hefte, Reihe A, **19(6)**, 159–186.

PACES, J.B. & MILLER, J.D. 1993. Precise U–Pb ages of Duluth Complex and related mafic intrusions, northeastern Minnesota: geochronological insights to physical, petrogenetic, paleomagnetic, and tectonomagmatic process associated with the 1.1 Ga Midcontinent Rift System. *Journal of Geophysical Research*, **98**, 13997–14013.

PANKHURST, R.J., RAPELA, C.W., SAAVEDRA, J., BALDO, E., DAHQUIST, J., PASCUA, I. & FANNING, C.M. 1998. The Famatinian magmatic arc in the central Sierras Pampeanas: an Early to Mid-Ordovician continental arc on the Gondwana margin. *In:* PANKHURST, R.J. & RAPELA, C.W. (eds) *The Proto-Andean Margin of Gondwana*. Geological Society, London, Special Publications, **142**, 343–367.

PANKHURST, R.J., RAPELA, C.W. & FANNING, C.M. 2000. Age and origin of coeval TTG, I- and S-type granites in the Famatinian belt of NW Argentina. *Transactions of the Royal Society of Edinburgh, Earth Sciences*, **91**(1/2), 151–168.

PANKHURST, R.J., RAPELA, C.W., LOSKE, W.P., FANNING, C.M. & MÁRQUEZ, M. 2003. Chronological study of the pre-Permian basement rocks of southern Patagonia. *Journal of South American Earth Sciences*, **16**(1), 27–44.

RAPELA, C.W., COIRA, B., TOSELLI, A. & SAAVEDRA, J. 1992. The Lower Paleozoic magmatism of southwestern Gondwana and the evolution of Famatinian orogene. *International Geology Review*, **34**, 1081–1142.

RAPELA, C.W., PANKHURST, R.J., BALDO, E., CASQUET, C., GALINDO, C., FANNING, C.M. & SAAVEDRA, J. 2001. Ordovician metamorphism in the Sierras Pampeanas: new U–Pb SHRIMP ages in central–east Valle Fértil and the Velasco Batholith. *In:* EDITOR, A. (ed.) *III South American Symposium on Isotope Geology, Extended Abstracts Volume (CD)*. Sociedad Geológica de Chile, Santiago, 616–619.

STEIGER, R.H. & JÄGER, E. 1977. Subcommission on geochronology: convention on the use of decay constants in geo- and cosmochronology. *Earth and Planetary Science Letters*, **36**, 359–362.

TERA, F. & WASSERBURG, G. 1972. U–Th–Pb systematics in three Apollo 14 basalts and the problem of initial Pb in lunar rocks. *Earth and Planetary Science Letters*, **14**, 281–304.

THOMAS, W.A. & ASTINI, R.A. 2003. Ordovician accretion of the Argentine Precordillera terrane to Gondwana: a review. *Journal of South American Earth Sciences*, **16**, 67–79.

TORO, B.A. & BRUSSA, E.D. 1997. Graptolitos de la Formación Suri (Arenig) en el Sistema de Famatina, Argentina. *Revista Española de Paleontología*, **12**, 175–184.

TOSELLI, A.J., SAAVEDRA, J. & ROSSI DE TOSELLI, J.N. 1996. *In:* ACEÑOLAZA, F., MILLER, H. & TOSELLI, A. (eds) *Geología del Sistema de Famatina*. Münchner Geologische Hefte, Reihe A, **19(6)**, 283–291.

SAAVEDRA, J., TOSELLI, A., ROSSI, J., PELLITERO, E. & DURAND, F. 1998. The Early Palaeozoic magmatic record of the Famatina System: a review. *In:* PANKHURST, R.J. & RAPELA, C.W. (eds) *The Proto-Andean Margin of Gondwana*. Geological Society, London, Special Publications, **142**, 283–295.

WILLIAMS, I.S. 1998. U–Th–Pb geochronology by ion microprobe. *In:* MCKIBBEN, M.A., SHANK, W.C. III & RIDLEY, W.I. (eds) *Applications of Microanalytical Techniques to Understanding Mineralizing Processes*. Reviews in Economic Geology, **7**, 1–35.